Flashover Current Pulse Formation and the Perimeter Theory

Dale C. Ferguson and Boris V. Vayner

***Abstract*— Electrostatic discharges on the spacecraft solar array surfaces have been studied for over 40 years. Multiple tests in many laboratories have been performed to reveal the mechanisms of current pulse formation, to determine plasma expansion speed and dimensions of neutralized surface area, and to define the parameters of the electric circuits to be able to adequately simulate space discharges in plasma chambers. Initially, a thorough analysis of all the available experimental data is performed to achieve progress in the creation of a satisfactory theoretical description of pulse wave forms and surface neutralization processes. It is shown that there are two main reasons for the significant variations observed in pulse wave forms, durations, and amplitudes; differences in test arrangements and pure statistical variations caused by the random nature of arc inception and development. Then, the theoretical model of flashover current pulse formation due to coverglass charge neutralization at the plasma perimeter is carefully considered and confronted with existing experimental data. It is found that this theory contains some appropriate elements but cannot be applied for quantitative explanation of pulse wave forms. The comparison of theoretical results and experimental data clearly shows that there is no (and there cannot be) such thing as a standard pulse. To estimate the possibility of detrimental effects from primary arcs, these events must be studied and analyzed statistically.**

***Index Terms*— DC electric field measurements, spacecraft charging.**

NOMENCLATURE

C	Capacitance per unit area (F/m^2).
E	Electric field strength (V/m).
H	Array width (m).
I	Current (A).
L	Distance (m).
Q	Electric charge (C).
R	Distance from arc (m).
S	Area (m^2).
T_e	Electron temperature (eV).
U	Voltage (V).
d	Thickness of coverglass (m).
j_F	Fowler–Nordheim current density (A/m^2).
h	Height of protrusion (m).
l	Array length (m).
n_e	Electron number density (m^{-3}).
r	Radius of protrusion (m).
t	Time (s).
β	Field enhancement factor.
ε	Dielectric permittivity.
ε_0	Permittivity of free space.
υ	Plasma front speed (m/s).
ν_c	Collision frequency (s^{-1}).
ρ_m	Metal density (kg/m^3).
ρ_e	Bulk resistivity (Ωm).
σ	Surface charge density (C/m^2).
τ	Pulsewidth (s).
τ_e	Explosion time (s).

Manuscript received August 23, 2012; revised February 19, 2013 and July 16, 2013; accepted August 20, 2013. Date of publication September 9, 2013; date of current version December 9, 2013.

D. C. Ferguson is with the Air Force Research Laboratory, Space Vehicles Directorate, Kirtland AFB, Albuquerque, NM 87117 USA (e-mail: dale.ferguson@kirtland.af.mil).

B. V. Vayner is with the Ohio Aerospace Institute, Cleveland, OH 44142 USA (e-mail: boris.v.vayner@nasa.gov).

Color versions of one or more of the figures in this paper are available online at http://ieeexplore.ieee.org.

Digital Object Identifier 10.1109/TPS.2013.2279760

I. INTRODUCTION

IT IS well known that arc-current pulse wave forms and pulse energies depend on the size of the sample, and that is why various test circuitry modifications have been suggested to better simulate discharges on a large wing in ground-based plasma chambers. The problem is clear—modern solar array wings have areas in the order of 10 m^2 while most of the plasma test chambers can only accommodate samples with areas <1 m^2. To resolve this long standing dilemma, a number of large-scale tests have been conducted in ground-test facilities during the last several years [1]–[4]. Thorough analysis of arc-current pulse parameters measured in different laboratories have revealed significant statistical variations in pulse wave forms, durations, and amplitudes.

Comparative study of the collected data records allows the establishment of strict limits on peak currents, and shows that pulse waveforms usually differ considerably from the perimeter theory developed in [2]. Essentially, array dimensions determine just the possibility of extremely long duration discharges, but the majority of events are characterized by pulse parameters that depend on the arc-site properties and the magnitude of differential charging. This conclusion explains the large and significant statistical scatter observed in the recorded data. Detrimental effects of primary arcs are estimated as negligible for all the solar cell types used in space applications to date.

II. THEORETICAL MODEL

Differential charging of a solar array coupon in a vacuum chamber is achieved by charging the semiconductor layers with an external power supply and generating a positive charge

0093-3813 © 2013 IEEE

on coverglass surfaces by irradiating them with energetic electrons.

A (quasi)-steady-state situation can be described as follows: the potential of semiconductor layers is equal to the bias voltage U_b (a few kilovolts negative), and the coverglass potential U_{cg} is more positive than U_b. Thus, the differential charging

$$U_{\text{diff}} = U_{cg} - U_b \tag{1}$$

reaches the magnitudes of 0.8–2 kV depending on a solar array material and design. The electric field inside the coverglass dielectric is given by

$$E_{\text{in}} = \frac{\sigma_1 + \sigma_2}{2\varepsilon\varepsilon_0} = \frac{U_{\text{diff}}}{d} = 1 - 4 \text{ MV/m} \tag{2}$$

where the numerical results above are from the measurements. From Gauss's law, we can write the electric field above the coverglass

$$E_{\text{out}} = \frac{\sigma_1 - \sigma_2}{2\varepsilon_0} = 1 - 0.3 \text{ kV/m} \tag{3}$$

where the numerical results came from measurements made with a TREK probe with its head 3 mm from the coverglass surface and U(TREK) $-U_{cg}$ = 1–3 V (note the accuracy of these measurements). It follows from these two equations that

$$\sigma_1 + \sigma_2 = \varepsilon \left(10^3 - 10^4\right)(\sigma_1 - \sigma_2) \tag{4}$$

and so $\sigma_1 \approx \sigma_2$. Thus, the total charges on the coverglass and semiconductor below are almost exactly equal

$$Q_{cg} = \int \sigma_1 dS \approx Q_{sc} = \int \sigma_2 dS. \tag{5}$$

One of the very important conclusions follows from (5): a complete discharge of the coverglass surface during an arc can only be possible in the special case when the loss of negative charge to the external structures is excluded. Of course, this is approximately true when there is low additional capacitance (C_{ext}, where in ground-based experiments C_{ext} is the capacitance in the bias circuit, but in space, it is the spacecraft capacitance to space)

$$C_{\text{ext}} \ll \frac{Q_{cg}}{U_b}. \tag{6}$$

For a 100-μm coverglass thickness, the inequality (6) can be written as follows:

$$C_{\text{ext}} \ll 0.25 \cdot S \cdot \frac{U}{U_b}\,\mu F \tag{7}$$

where S is in m^2, and this inequality has been valid for all the plasma cloud expansion experiments performed to date.

When an arc occurs, the plasma cloud starts to expand, and free electrons from the plasma cloud neutralize positive charges on the coverglasses. Electrons move from the semiconductor layer to the arc site, then to the plasma, and then to the coverglass and the chamber structure, closing the current loop. According to perimeter theory [2], the magnitude of the pulse current can be written as follows:

$$I(t) = CU\frac{ds}{dt}. \tag{8}$$

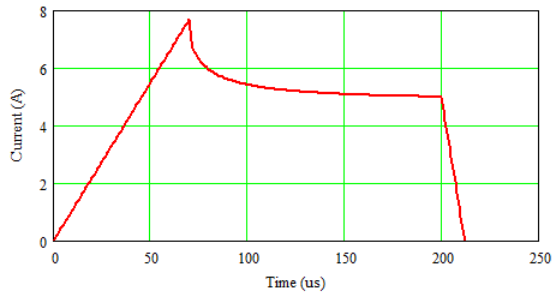

Fig. 1. Predicted current pulse wave form. Coupon dimensions 1.4 m × 4 m, arc in the center, v = 10 km/s, and U = 800 V.

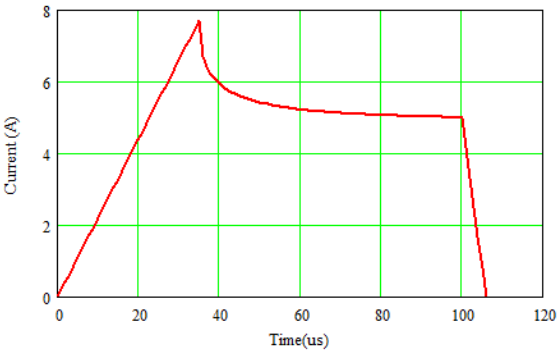

Fig. 2. Predicted pulse wave form for the same sample. Expansion speed v = 20 km/s and U = 400 V.

If the arc occurs in the geometrical center of a rectangular coupon, (8) takes the following form:

$$I(t) = 2\pi CUv^2 t; \quad t \le \frac{H}{2v}$$
$$I(t) = 4CUv^2 t \cdot a\sin\left(\frac{H}{2vt}\right); \quad t > \frac{H}{2v}. \tag{9}$$

Arc-current pulse wave forms for this particular case are shown in Figs. 1 and 2. The current was calculated for a solar array with a capacitance per unit area of C = 0.25 μF/m^2, and differential charging of U = 800 and 400 V, respectively.

To compare the graphs in Figs. 1 and 2 with available measurements, the current contribution from the arcing string should be subtracted. However, the area of one string is much smaller than the area of the entire coupon, so these graphs are expected to resemble the observed ones. Perhaps surprisingly, the only published example of a good qualitative resemblance between the measured pulse wave forms and those shown in Figs. 1 and 2 was reported in [2] for an array of 133 cm × 59 cm dimensions and 800 V differential charging. Even then, the difference between the calculated and measured currents reached 25%–100% [2].

It can be observed that the peak current depends on the plasma expansion speed and the differential voltage, whereas the pulsewidth is determined by the plasma front propagation time. These results were obtained for constant plasma expansion speed. However, imaging the flashover propagation with an IR camera demonstrated a decreasing speed ($v \sim t^{-1/2}$) [5]. Measurements of plasma propagation time over the surface of one string also showed a decreasing speed [6].

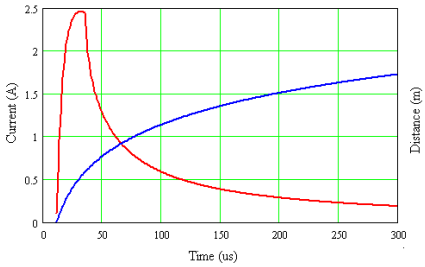

Fig. 3. Arc-current pulse wave form computed for the 1.4 m × 4 m sample with differential voltage of 400 V.

If the plasma expands as $R(t) = R_0(t/t_0)^{\alpha}$, then the current is

$$I\,(t) = 2\pi CU\alpha \frac{R_0^2}{t_0^{2\alpha}} t^{2\alpha-1}. \tag{10}$$

It follows from (10) that the current increases linearly in the case of constant speed [$I(t) \sim t$ when $\alpha = 1$], but the current pulse has a plateau region ($I = \text{const}$) when $\alpha = 1/2$. A rich ensemble of measurements concerning plasma propagation was obtained and analyzed in [7], where the best fit relation was computed and presented as

$$R\,(m) = -1.32 + 1.23 \log t\,(\mu s)\,. \tag{11}$$

Even though the statistical dispersion was significant, relation (11) pointed to a slower decrease in plasma speed compared with the earlier results [5], [6]: $v \sim t^{-1/4}$. Substituting (11) into (8), one can compute the expected current pulse wave form (Fig. 3).

Thus, simulations of current pulse wave forms within the framework of the perimeter theory result in the prediction of peak current magnitudes of 3–8 A, effective pulsewidths of a few hundred microseconds, and some kinds of plateau regions in the pulse evolution history. It should be noted that theoretical wave forms were obtained under the assumption of complete surface discharge. Real measurements show that such events have a very low probability on the order of 1% [7].

The electrostatic discharge (arc) is initiated by a thermal explosion of a tiny protrusion on a conductor (semiconductor) surface [8]. The metal plasma ball created expands with a high speed that can be calculated as [9]

$$v = \left(\frac{4\gamma}{\gamma - 1} w_0\right)^{1/2}. \tag{12}$$

Ohmic losses of electric current caused by the field emission process deliver heat to the atoms of metal. In this case, the specific energy is

$$w_0 = \beta \frac{E \cdot j_F}{\rho_m} \tau_e. \tag{13}$$

For monoatomic silver metal plasma ($\gamma = 1.67$) and explosion time $\tau_e = 1$–10 ns [8], an estimate for plasma expansion speed is

$$v = (0.7 - 2.2)\,\beta^{1/2}\,\text{km/s}\ . \tag{14}$$

The field enhancement factor β can be calculated from the Fowler–Nordheim formula that relates electric field strength, work function, and field emission current density [6]. For an electric field strength of 10^7 V/m, this factor is $\beta \approx 100$. Thus, the plasma expansion speed is estimated to be from 7 to 22 km/s, in very good agreement (factor ≈ 2) with the experimental data obtained in [10] for vacuum arcs on a silver cathode.

One more argument in favor of a thermal nature for a protrusion explosion is the independence of ion speed on ion charge [10]. Thermal explosions of thin silver wires were studied in [11]. The rate of vaporization for wires with diameter ~20 μm was measured by two different methods and determined as (4.5 ± 0.4) and (3.8 ± 0.3) km/s, respectively. This means that the explosion time for a protrusion with a diameter of 1–10 μm can be estimated to be 0.2–2 ns. However, the specific energy in experiments [11] was a few times lower than our estimate (13), and may be caused by the difference in current densities in long wires and small protrusions. The amount of evaporated silver ($m \sim r^2 h$), field enhancement factor ($\beta \sim h/r$), and time of explosion depend on the random magnitudes of the protrusion dimensions. That is why significant variations in observed plasma expansion speeds and discharged areas are reported in all of the relevant publications.

Another complication emerges from the obvious fact that the plasma expands into the space with a very inhomogeneous electric field. Conductive elements of the chamber structure have zero potential, whereas coverglasses on nonneutralized cells have a positive potential up to 1 kV with respect to the arc site. The influence of this spatial potential distribution on the plasma expansion rate can be determined by comprehensive experiments and computer simulations, which are well beyond the scope of this paper.

However, there are some arguments in favor of significant shielding of the electric field by the expanding plasma. The electron number density at a distance of ~1 m from the arc site was estimated as $n_e = 10^7$–10^8 cm^{-3} [6]. Comparable results [11] were obtained by the optical measurements of plasma density. The Debye length

$$\Lambda_D = \left(\frac{T_e}{4\pi n_e e^2}\right)^{1/2}$$

is <1 mm for a plasma with an electron temperature of 3–6 eV, typical for a vacuum arc plasma. Thus, the ratio of Debye length to the plasma cloud radius stays small and constant during the plasma expansion into the vacuum ($n_e \sim R^{-2}$). Debye shielding does not allow the electric field to penetrate deeply into the plasma and influence the current density spatial distribution. However, edge effects may be significant, considering the very high ratio of U/T_e. This problem needs further investigation.

To validate this theory, it is necessary to compare the predicted pulse wave forms with discharge pulses recorded in the laboratory.

III. Experimental Results

The best published agreement between the simulated and measured wave forms for the perimeter theory was demonstrated in [2] and is shown in Fig. 4. The theoretical curve

corresponds to the measurements in terms of duration and dissipated charge but deviates significantly in the areas of the pulse front and pulse tail. Peak currents also differ by 20%–25%. It should be noted that the statistical dispersions of pulse parameters were comparable with the averages [2, Table II]. In such a case, the attempt to introduce a standard pulse wave form seems to be very doubtful. To elucidate the deficiencies in the theory, one particular case is analyzed below.

A large area coupon (133 cm × 59 cm) was used for this test. The coupon consisted of 19 strings with 16 cells each, was mounted horizontally in a vacuum chamber of 1.85-m diameter and 3-m length, and all the strings were biased to −5 kV, providing a differential potential of 800 V. In one case of a long-lasting discharge, the arc site was located in the middle of string #9. In reality, the current from the arcing string should be added to the theoretical curve in [2, Fig. 17], which implies a flashover discharge of string #9 with a plasma expansion speed of 7.7 km/s and a differential voltage of 800 V

$$I_9 = CU \cdot lv \approx 0.095\,A$$

and the pulse front duration was $\tau_f = 39\,\mu s$.

The neighboring string #10 shows a peak current of 0.3 A, a discharge front time of 7 μs, and discharges fully in 50 μs. The capacitor discharge current was not shown in [2], but it is easy to compare the capacitor charge with the electrical charge accumulated by one string

$$Q_c = C_{\text{ext}} V_b = 1.65\,\mu C, \quad Q_s = CUS_s = 6.9\,\mu C. \qquad (15)$$

The external capacitance was estimated as $C_{\text{ext}} = 330$ pF.

The peak current can be estimated as

$$I_p = \frac{2Q}{\tau}. \qquad (16)$$

If the capacitor discharge time is ∼5 μs, then the peak current reaches 0.6 A and is comparable with the measured current during the initial 3–5 μs of the discharge. The estimate for a string current brings the magnitude to 0.3 A, in an excellent agreement with the measurements. Thus, the perimeter theory explains the total lost charge quite accurately, but fails to explain the pulse wave form. For example, the difference between the calculated and measured peak currents is ∼25%, and it is almost 100% for the falling branch (tail) of the current pulse wave form.

Another experiment with a large area coupon was reported in [1]. A bias voltage of −8 kV was applied to all 12 strings containing 19 cells each (75 cm × 75 cm coupon). The coupon was mounted in an acrylic chamber of 2-m diameter and 2-m height. The external capacitance was estimated at 625 pF. A Langmuir probe was mounted 1 m from the coupon. Two examples of measured discharge current pulses and linear programming (LP) signals are shown in Figs. 7–9 [1]. The peak current reached 3 A (0.3 μs) without an external capacitor, and 3.6 A (2 μs) with a 500-pF capacitor. Similar pulse forms were obtained for a 40 cm × 40 cm coupon in a stainless steel chamber [8]. The peak current was close to 1.5 A (<5 μs) with an estimated 100-pF external capacitance.

Fig. 4. In this presented best fit, the rising and decaying pulse wave forms are poorly fit, whereas the total charge is fairly well represented [2].

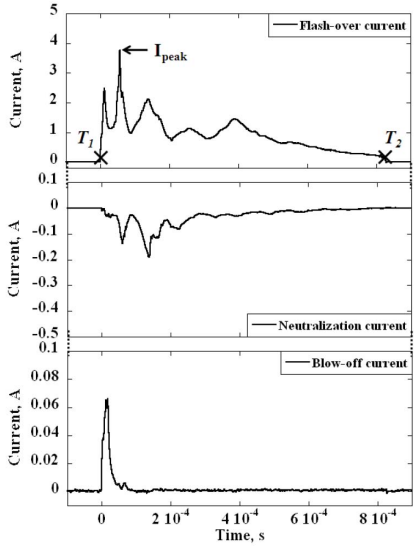

Fig. 5. Largest amplitude and longest arc found in [7]. Note the complicated waveform, in essential disagreement with perimeter theories.

The largest coupon tested to date was a 1.2 m × 4 m panel with 24 strings containing 700 3J cells [7]. This coupon was installed in a large chamber (2-m diameter and 5-m length), biased to −5.5 kV, and charged differentially up to 1 kV. An external capacitor of 240 pF was connected in parallel with the power supply. The longest duration pulse obtained is shown in Fig. 5. The peak current reached 3.7 A (30–70 μs), and the pulse duration was >800 μs. It should be noted that the statistical spread of arc-current pulse parameters was very large [7, Fig. 14]. After recording and analyzing 350 events, the authors found that 255 events resulted in neutralizing less than half of the array area, and only one event neutralized almost the whole array.

These measurements create doubts about the validity of the perimeter theory—surface charge is still available, yet the discharge extinguishes itself. The attempt to determine the plasma expansion speed yielded a statistical trend (11), but applying this formula to the simulation of pulse wave forms within the framework of perimeter theory resulted in an essential disagreement between the simulated (Fig. 3) and observed forms (Fig. 5).

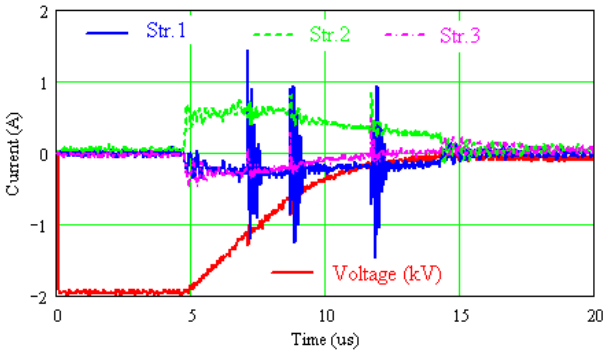

(a)

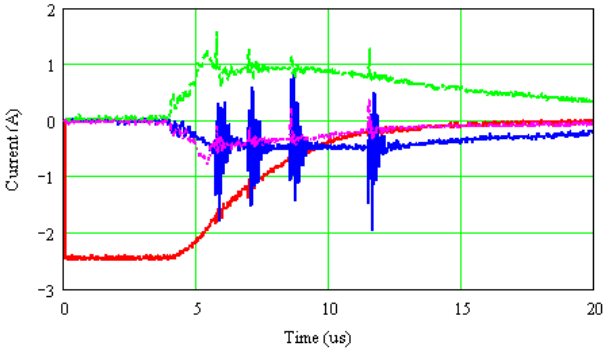

(b)

Fig. 6. Rise time of arc-current pulse was very short. (a) Array potential dropped to zero but not to the coverglass potential. Differential charging reached 0.8 kV. (b) Front of arc-current pulse was ~2 μs. The array potential dropped to zero but not to the coverglass potential. Differential charging reached 1.1 kV.

TABLE I
PULSE CHARACTERISTICS FOR 10 ARCS IN A GEO SIMULATED ENVIRONMENT (STANDARD DEVIATIONS ARE IN PARENTHESES)

Expt No	Beam Energy (keV)	Bias (kV)	Peak curr (A)	Front (us)	Pulse width (us)	Lost charge (uC)	Number of events
1	2.6	-2	0.63(0.15)	0.14(0.02)	12.2(3)	3.8(0.9)	5
2	3.3	-2.5	1.03(0.13)	0.99(0,8)	14.8(3)	7.4(1.6)	5

Experiments with low-area samples have revealed some essential features of a discharge in vacuum [6]. In these experiments, the only additional capacitance was a high-voltage probe (300 pF). Two examples of such current and voltage pulses are shown in Fig. 6.

Statistical analysis of 10 events from these experiments is shown in Table I.

The capacitor discharge time was ~10 μs, and it discharged to ground potential. The flashover current pulse had a time interval of ~5 μs when the current did not change. This implies a decreasing plasma expansion speed

$$v = 25 \cdot t^{-1/2}\,\mathrm{km/s}\ . \tag{17}$$

A similar dependence of expansion speed on time was found in [5] for a relatively small (40 cm × 40 cm) coupon. One more interesting observation is that the pulse wave forms are similar in all the publications reviewed above except [2]. Measurements of expansion speed performed for high-current vacuum arc plasmas reveal some decrease in speed with time but the dependence was much slower than in (7) [13]. The arc plasma expands in all possible directions with a speed of ~10–20 km/s. The plasma front reaches the tank wall or closest grounded conductive element of the chamber in a time interval of

$$\Delta t = \frac{L}{v}. \tag{18}$$

Thus, the potential of the arc site drops to the ground potential within a time interval shorter than 30 μs, depending on the plasma chamber design and experimental setup.

The peak current is determined by two different items: 1) the external capacitance and bias voltage and 2) differential charging and the array surface capacitance [see (2)].

The relatively low magnitudes of peak currents in experiments [1]–[7] can be explained by small external capacitances used in these experiments. Spacecraft capacitances may vary within a wide range, depending on the spacecraft size and design, but do not exceed a few thousand picofarads. The probability of solar cell damage caused by a primary arc is an increasing function of the peak current and peak arc pulse power [15], [16].

To induce measurable degradation to a solar cell, the primary arc site should be located on the cell edge and the peak current should be well over 10 A for triple junction cells and significantly higher for silicon cells [15], [16]. In other words, additional capacitances should be ~0.5–1 μF, which are much higher than the estimated spacecraft capacitances. Decreasing the peak current and increasing the pulsewidth by incorporation of an additional resistor in the discharge circuit results in a significant decrease in the probability of cell damage. In addition, the majority of discharges occur on the interconnectors between cells, and these discharges do not produce detrimental consequences.

There are solar array designs with no exposed interconnects, such as the ISS solar cells with welded through interconnects. This seems to be useful for studying arc inception and arc plasma propagation on such an array sample. We report here on one such test. The coupon tested consisted of six strings with 12 cells (8 cm × 8 cm) in each string. The coupon was biased negatively through an RC circuit ($R = 100\,\mathrm{k\Omega}$ and $C =$ 3.2 nF) and irradiated with an electron flux of 0.8–1 nA/cm^2. Differential charging reached 1 kV. Current pulse wave forms were recorded for four strings. One example of discharge on cell edge in the middle of a central string is shown in Fig. 7.

It is observed in Fig. 7 that the total current pulsewidth was $\tau_f = 75$ μs, while the capacitor was fully discharged much faster—$\tau_C = 26$ μs. The contribution to the peak of the measured flashover current from the external capacitor can be estimated as

$$I_C = \frac{2C_{\mathrm{ext}}U_b}{\tau_c} \approx 1\,A. \tag{19}$$

Thus, the contribution to the flashover current from the external capacitor was negligible only 20 μs after discharge initiation. If we suggest that the flashover current was caused by the plasma expanding to the edge of the coupon then the

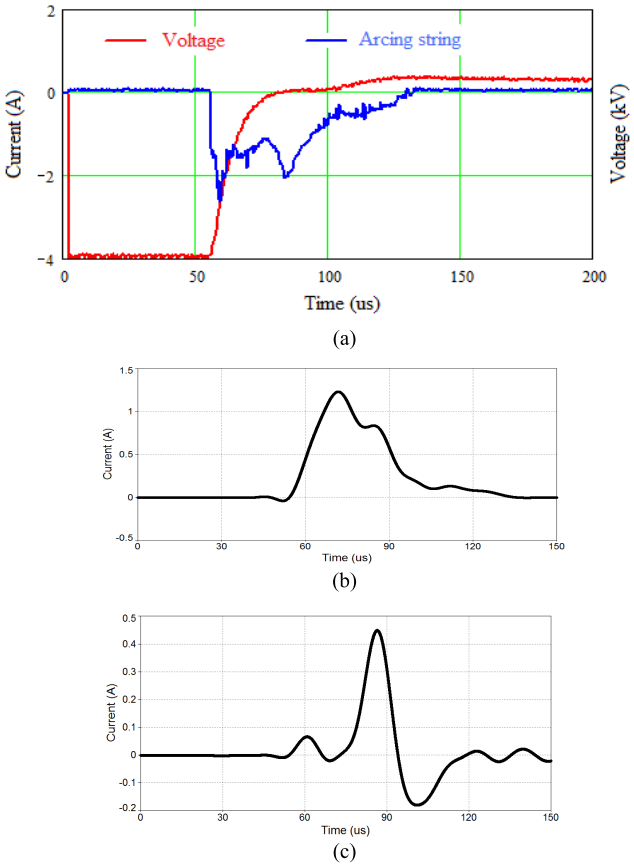

Fig. 7. Flashover current and voltage pulse wave forms are shown for an arc in the center of the coupon. Arc initiation times on (b) and (c) should be shifted to coincide with that in (a). (a) Voltage and current on arcing string, (b) current on adjacent string (smoothed), and (c) current on farthest string (smoothed).

average speed was

$$\bar{v} = \frac{L}{\tau_f} = 9.3\,\text{km/s}. \tag{20}$$

Substituting the magnitude of speed from (20) into (9) results in an expected flashover current of ~4.5 A that is at least two times higher than the recorded value. One possible explanation for this discrepancy can be given by the partial discharge of coverglass surfaces. TREK probe scans performed just after the discharge revealed a residual differential voltage of 200–500 V. Another estimate for plasma expansion speed was obtained from the voltage pulses on the Langmuir probes. The discharge current reached a peak at 60 μs, positive peaks on LPs were reached at 136.6 and 135.8 μs, distances from the arc site were 74.6 and 72 cm (LP3 and LP2), and the speed could be calculated as 9.7 and 9.5 km/s. Altogether, data processed in this way show a speed of ~10 km/s. It would be good if all the data were reproducible as shown in this example, but statistical analysis of 33 events demonstrated a huge dispersion in all pulse parameters.

The most striking instance was two arcs located on the same spot, but with very different recorded wave forms. This observation perfectly shows the random nature of the plasma creation and expansion. It is worth noting that arcs on this coupon generated plasmas from silicon and/or germanium but not from silver, as might be expected for a solar array with no exposed interconnects.

IV. What Is the Current-Limiting Factor?

The flashover arc-current circuit in GEO only contains four different elements.

1) The capacitance of the ground-to-coverslide.
2) The circuit wiring to the arc site.
3) The arc site itself and the plasma generation process.
4) The plasma generated at the arc site that expands over and discharges the coverslides.

When an ESD event occurs, the energy and charge stored in the capacitance to space (or to the vacuum chamber wall) is released quickly (the blowoff current) and the arc site approaches the ambient plasma potential. Because of capacitive coupling, this places the surface of the coverslides at a positive potential equal to the differential potential that existed before the ESD.

Usually, the energy stored in the coverslide capacitance is fixed by the controlled differential potential between the coverslide surfaces and the arc site. As the plasma expands out to discharge the coverslides, charge is neutralized on the coverslide surface, and is therefore instantaneously released from the other side of the capacitance (i.e., the solar array ground) and travels to the arc site, where it melts, vaporizes, and ionizes the material that will be the expanding arc plasma. This plasma then expands out to continue discharging the coverslide surfaces.

Thus, the only possible current-limiting factors are the following.

1) The resistance of the arc plasma between the arc site and the point of coverslide discharge.
2) The coverslide neutralization rate because of the speed of plasma expansion and the degree of neutralization at each point on the coverslides.
3) The resistance of the circuit leading the current back to the arc site.
4) The melting, vaporization, and ionization process.

Below, we treat each of these current-limiting factors in turn.

Factor 1: Plasma resistivity does not limit peak current in our small arcs—this was confirmed by experiments with a large external capacitance of 1 μF [14], [15]. The current reached 50–70 A in 20–30 μs after the discharge inception, implying a current-limiting resistance of perhaps 10 Ω, compared with the ~(500 V/5 A) ~100-Ω current-limiting resistance in the low-capacitance experiments. This is understandable in terms of theoretical values for plasma resistivities. Taking the resistivity of a plasma [18] to be

$$\rho = \frac{1}{4\pi\,\varepsilon_0} \cdot \frac{\nu_e}{\omega_p^2} (\Omega \cdot m) \tag{21}$$

where ω_p is the plasma frequency and ν_e is the electron collision frequency, and

$$\nu_e^{-1} = \frac{3}{4} \cdot \frac{m_e^{1/2}}{\sqrt{2\pi}} \cdot \frac{(kT_e)^{3/2}}{e^4 n_e \Lambda} \tag{22}$$

and here

$$\Lambda = \ln\left(\frac{(kT_e)^{3/2}}{e^2(4\pi ne^2)^{1/2}}\right)$$

is the Coulomb logarithm. From the vacuum arc measurements [8] and our spectral measurements, the electron temperature is estimated to be within the 4–6-eV range. It can be observed from Fig. 9 that Λ varies within limits of 10–20.

After simple algebra, the resistivity can be written as

$$\rho = \frac{\sqrt{2\pi}}{4\pi^2\varepsilon_0}\cdot\frac{e^2m_e^{1/2}}{(kT_e)^{3/2}}\Lambda = 2.5\cdot 10^{-5}T_e^{-3/2}\Lambda\ \ \Omega\cdot m \quad (23)$$

where the electron temperature is expressed in electron volts.

From our experiments, the peak current was achieved at τ = 1–10 μs. The plasma front position can be calculated as

$$l = v\cdot\tau. \quad (24)$$

If the plasma expansion speed was v = 10 km/s, then l = 1–10 cm, and the plasma resistance was

$$R \approx \rho l/A$$

where A is the area being discharged $\approx \pi l^2$

$$R \approx 8 - 80\ m\Omega. \quad (25)$$

This is three orders of magnitude less than the $\sim$100 Ω needed, and therefore the bulk plasma resistance cannot be the current-limiting factor.

Factor 2: The current limitation of the arc-plasma expansion can be found from (8)

$$I(t) = 2\pi CUv^2t\,;\quad t \le \tfrac{H}{2v}\,.$$

Here, from Ohm's law, the effective resistance $R = U/I = 1/(2\pi Cv^2t)$. As mentioned above, this can give peak currents similar to what are observed in some instances (see Fig. 4), but overpredicts the current by a factor of two or so in other instances [see Fig. 7(a)]. Perhaps of most concern is that even when the peak current is approximately correctly predicted, the observed pulse wave form is sometimes above and other times below that predicted, and in some cases has several peaks separated by tens of microseconds. Let us assume that the current predicted by the perimeter theory is above that measured. This could easily be explained by an incomplete discharge of the coupon at that time in the pulse. However, if the predicted current is below that measured, we are somehow discharging more capacitance than the sample has available! In other words, it is unlikely that the capacitance discharged at the perimeter of the expanding plasma can be the current-limiting factor. Something else must be limiting the current, and thus the current predicted by the arc-plasma expansion can only be considered an upper limit to the real current.

Factor 3: The circuit resistance is at most a few ohms, because it is purposely minimized to obtain maximum current from the array. Thus, it cannot be the current-limiting factor.

Factor 4: Melting, vaporization, and ionization at the arc site. It is clear that during an arc, the production of the arc plasma will be a dynamic process. It depends sensitively on the temperature at the arc site, since it is this temperature that produces melting and vaporization. The temperature, in turn, depends on the current flowing and on the area through which that current flows. If the arc site is a whisker or rough spot, the geometry of the arcing site may change as the whisker gets eaten away. The ionization depends sensitively on the electric field at the arc site, and thus on the geometry as well. If the arc site at a given time is smooth, the edges of the crater formed may sharpen with time, concentrating the field, and thus concentrating the electron acceleration regions. One can also imagine (and we can observe in vacuum chambers!) that sometimes molten metal is blown off the arc site and can drastically change the energy balance and geometry of the arc site. If the arc site has a strong electric field, the plasma temperature may be elevated, and the expansion velocity will be higher, and so on.

Another ubiquitous characteristic of the solar array arcs must be mentioned here. Pulse waveforms obtained in [17] show that contrary to expectation from the perimeter theory, current initiation occurs approximately simultaneously on all strings and continues until it is rapidly extinguished simultaneously on all strings (so rapidly that it causes ringing in the measurement circuit). That is, the initiation and extinguishing of the arc current seem to be more a function of what is happening at the arc site (thresholds being reached, perhaps) than exactly where the arc-plasma perimeter is and how much charge it is capable of neutralizing. All of this is to say that the changing characteristics of the arc site can explain the multitude of pulse wave forms and timescales observed, as well as the rapid and simultaneous shutdown of the arc current on all array strings. It seems most likely, then, that the current limitations of the melting, vaporization, and ionization process are the dominant current-limiting process.

Some authors [19] claim that the simultaneous turn-on of current in all array strings is the result of a burst of fast electrons from the arc site reaching all of the strings practically simultaneously. These electrons must be space-charge limited, and moving at such high speed that they reach all parts of the array on a submicrosecond timescale. From [19], "when the electron reaches a dielectric at 500 V, its energy is $\sim$500 eV. This is equal to a velocity of 3×10^7 m/s for the fastest electrons." However, as the electric field at the dielectric is closely normal to the surface, and the acceleration of the electrons is only in that direction, the electron velocity along the surface (in the direction of the plasma expansion velocity we are talking about here) is not accelerated, and the potential of the surface is not at all germane to the discussion. Although it is well known that every ESD event on solar arrays is preceded by a burst of high-speed electrons [20], they are blowoff electrons, which are lost from the array and cannot provide the observed flashover current in the solar array strings.

There are many reasons for skepticism about the fast electron idea. First, the electric field near the arc site will be greatly reduced by the initial blowoff current impinging on the adjacent dielectric surfaces (coverglass edges, etc.), so there will be no strong local electric field at the arc site to produce the fast electrons after that time. The blowoff current itself has no electric field drawing it back to the surfaces, so it cannot be the source of this immediate flashover

current. Second, electrons produced later in the arc must be produced thermally, and the thermal distribution will have only a tiny fast component due to electrons far out in the high energy tail. These can produce only negligible amounts of current. Third, because the blowoff current has brought the potential of the semiconductors very close to the potential of the chamber walls, there is no bulk electric field at the arc site, and the thermal electrons produced must then be restrained by the space charge of the positive ions (i.e., a plasma has been produced). Finally, the Debye length in the thermal plasma produced by the arc current is very small, and cannot permit electrons to extend far enough in the plasma to immediately impact the farthest strings. It is not the primary purpose of this paper to debunk the fast electron idea for the sudden simultaneous onset of the current in all the solar array strings, however, so we will leave further discussion to other papers.

Perhaps more credible as an explanation for the sudden onset of current simultaneously in all strings is the fact that as the capacitance to the chamber walls is discharged by the sudden burst of blowoff electrons and the arc site rises to near ground potential, all of the coverglass surfaces (which are tightly capacitively coupled to the semiconductors) suddenly go to high positive potentials and attract the extraneous electrons in the chamber. These could be electrons that were produced by photoemission on the coverglass (or other) surfaces, secondary electron emission from the incident electron-gun electrons, or in the case of LEO plasma test conditions, electrons from the ambient plasma in the chamber [21], [17]. In any case, the immediate net charge transfer will still be small compared with the total charge on the array but will affect all strings simultaneously.

A test of this idea under GEO conditions would involve eliminating all the sources of ionizing photons, turning the electron gun OFF after the desired differential potentials have been reached, and waiting for an arc. Then, photoemission and secondary electrons will not be a factor and the initial flashover current should be eliminated.

V. Fine Structure in the Arc Current

Further evidence of the importance of the arc-site conditions in limiting the current can be observed by examining the very fine structure of the current waveform. It can be observed in Fig. 8 that when measured with a very high time resolution, the capacitor current is extremely variable. Sometimes the current even goes to zero, followed nanoseconds later by recovery to a large amount. This can be understood in terms of a highly variable degree of ionized gas being produced at the arc site. As we have already mentioned above, the vacuum arc is a highly stochastic process, which proceeds by fits and starts, sometimes shutting down almost entirely only to come back on nanoseconds later in an adjacent spot [22]. This means that the smooth current waveform predicted by the perimeter theory must be only an upper envelope of the possible arc current, which accurately follows the array neutralization prediction when the vacuum arc is fully active, but falls to a fraction of the prediction when the arc site is mostly OFF. The stochastic

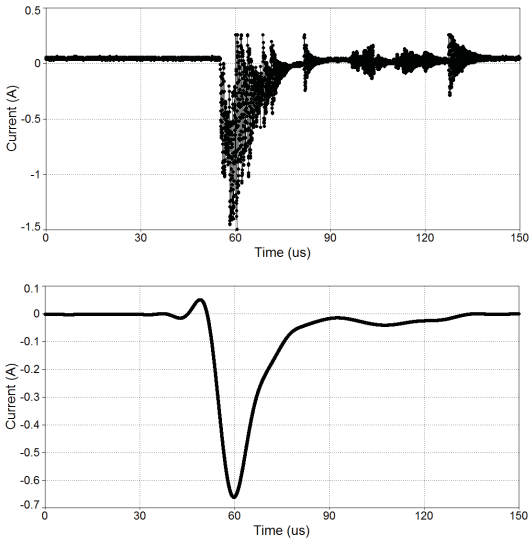

Fig. 8. Capacitor discharge current (top) and smoothed graph (bottom).

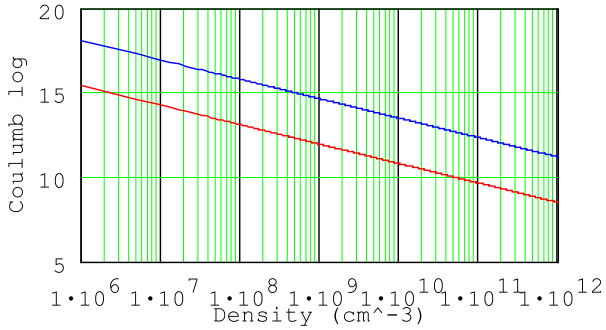

Fig. 9. Coulomb logarithm for electron temperatures of 1 eV (lower line) and 6 eV (upper line).

nature of the peak and total arc currents fits in well with this interpretation.

Summarizing the results of all tests conducted to date, one may deduce that primary arcs on a solar array surface are first initiated and later quenched on all strings simultaneously, exhibit peak currents <5 A, which occur early in the pulse, have long tails with low currents, and exhibit statistical dispersions in pulse characteristics of similar magnitude to the characteristics themselves. Many of these properties cannot be explained by the perimeter theory without modification to consider the instantaneous plasma-production conditions at the arc site. Current pulses with peaks of <5 A cannot cause any measurable degradation to the existing spacecraft power sources. However, the implementation of modern photovoltaic devices such as multijunction cells will certainly demand new comprehensive tests against cell degradation caused by the electrostatic discharges.

VI. Conclusion

Arc-current pulse parameters depend on many factors such as inception voltage, spacecraft capacitance, solar array area and specific capacitance, arc-site location, and cathode material electric and thermal properties. A number of experiments with large area solar array coupons in GEO simulated

environments have demonstrated that these parameters are characterized by very wide statistical distributions. Computer simulations of pulse forms based on a theory of surface discharge due to plasma propagation are more or less successful in matching integral characteristics of a discharge: total electric charge and pulsewidth. However, this theory fails in predicting the pulse wave forms and the fully neutralized area of the coverglasses.

A theory that considers the changing characteristics of melting, vaporization, and ionization at the arc site may explain the extreme variability of the current within an arc and between arc pulses. Because of this extreme variability, it is not rational to attempt to introduce a standard pulse to be generated in a laboratory test by deploying special electronics.

Statistical analysis of the measured data confirms that the peak current is always well <10 A, which means that primary arcs cannot inflict any important degradation on silicon and triple-junction solar cells. Other adverse effects of electrostatic discharges on solar array surfaces, such as electromagnetic interference, disruption of power supply function, and surface contamination should be considered and tested independently.

REFERENCES

[1] P. Leung, "Plasma phenomena associated with solar array discharges and their role in scaling coupon test results to a full panel," in *Proc. 40th Aerosp. Sci. Meeting Exhibit.*, 2002, AIAA-2002-0628.

[2] E. Amorim, D. Payan, R. Reulet, and D. Sarrail, "Electrostatic discharges on a 1 m^2 solar array coupon," in *Proc. 9th Spacecraft Charg. Technol. Conf.*, Tsukuba, Japan, 2005, p. 16.

[3] D. Sarrail, R. Reulet, V. Inguimbert, L. Levy, F. Boulay, and D. Payan, "Electrostatic discharge and secondary arcing on solar array," in *Proc. 10th Spacecraft Charg. Technol. Conf.*, Biarritz, France, 2007, p. 13.

[4] T. Okumura, M. Imaizumi, K. Nitta, and M. Takahashi, "Flashover discharge on solar arrays: Analysis of discharge current and image," *J. Spacecraft Rockets*, vol. 48, no. 2, pp. 326–335, 2011.

[5] H. Masui, K. Toyoda, and M. Cho, "Electrostatic discharge plasma propagation speed on solar panel in simulated geosynchronous environment," *IEEE Trans. Plasma Sci.*, vol. 36, no. 5, pp. 2387–2394, Oct. 2008.

[6] B. Vayner, D. Ferguson, and J. Galofaro, "Effect of solar array size on sustained arc inception," in *Proc. 47th AIAA Aerosp. Sci. Meeting Including New Horizons Forum Aerosp. Exposit*, 2009, AIAA-2009-0115.

[7] T. Okumura, K. Nitta, M. Takahashi, T. Suzuki, and K. Toyoda, "Flashover plasma characteristics on 5 m^2 solar array panels in a simulated plasma environment of geostationary orbit and low earth orbit," in *Proc. 48th AIAA Aerosp. Sci. Meeting Including New Horizons Forum Aerosp. Exposit*, 2010, AIAA-2010-1602.

[8] G. A. Mesyats, "Ectons and their role in plasma processes," *Plasma Phys. Control Fusion*, vol. 47, no. 2, pp. A109–A151, 2005.

[9] Y. B. Zel'dovich and Y. P. Raizer, *Physics of Shock Waves and High-Temperature Hydrodynamic Phenomena*. New York, NY, USA: Dover, 2002, p. 103.

[10] G. Y. Yushkov, A. Anders, E. M. Oks, and I. G. Brown, "Ion velocities in vacuum arc plasmas," *J. Appl. Phys.*, vol. 88, no. 10, pp. 5618–5622, 2000.

[11] M. Hu and B. R. Kusse, "Optical observations of plasma formation and wire core expansion of Au, Ag, and Cu wires with 0–1 kA per wire," *Phys. Plasmas*, vol. 11, no. 3, pp. 1145–1150, 2004.

[12] T. Kawasaki, S. Hosoda, J. Kim, K. Toyoda, and M. Cho, "Charge neutralization via arcing on large solar array in GEO plasma environment," *IEEE Trans. Plasma Sci.*, vol. 34, no. 5, pp. 1979–1985, Oct. 2006.

[13] S. Hohenbild, C. Grubel, G. Y. Yushkov, E. M. Oks, and A. Anders, "A study of vacuum arc ion velocities using a linear set of probes," *J. Phys. D, Appl. Phys.*, vol. 41, no. 23, p. 205210, 2008.

[14] B. V. Vayner, D. C. Ferguson, and J. T. Galofaro, "Comparative analysis of arcing in LEO and GEO simulated environments," in *Proc. 45th AIAA Aerosp. Sci. Meeting Exhibit*, 2007, AIAA-2007-0093.

[15] B. Vayner and L. Vayner, "Electrostatic discharges on triple junction solar cells in simulated LEO environment," in *Proc. 10th Spacecraft Charg. Technol. Conf.*, Biarritz, France, 2007, p. 16.

[16] T. Okumura, M. Cho, V. Ingumbert, D. Payan, B. Vayner, and D. Ferguson, "International round-robin tests on solar cell degradation due to electrostatic discharge," *J. Spacecraft Rockets*, vol. 47, no. 3, pp. 533–541, 2010.

[17] B. V. Vayner, D. C. Ferguson, R. C. Hoffmann, A. T. Wheelock, J. J. Likar, J. L. Prebola, Jr., D. H. Crider, T. A. Schneider, J. A. Vaughn, B. Hoang, K. Steele, S. Close, A. Goel, M. W. Crofton, J. A. Young, and J. M. Bodeau, "First preliminary results from U.S. round-robin tests," in *Proc. 12th Spacecraft Charg. Technol. Conf.*, Kitakyushu, Japan, May 2012, pp. 14–18.

[18] V. B. Baranov and K. B. Krasnobaev, *Hydrodynamical Theory of Space Plasma*. Moscow, Russia: Nauka, 1977, p. 31.

[19] V. Inguimbert, P. Sarrailh, J. C. Matéo-Vélez, J. M. Siguier, C. Baur, B. Boulanger, A. Gerhard, P. Pelissou, and D. Payan, "Measurements of the flashover expansion on a real solar panel (EMAGS3 project)," in *Proc. 12th Spacecraft Charg. Technol. Conf.*, Kitakyushu, Japan, May 2012, p. 6.

[20] J. T. Galofaro, C. V. Doreswamy, B. V. Vayner, D. B. Snyder, and D. C. Ferguson, "Electrical breakdown of anodized structures in a low earth orbital environment," NASA, Washington, DC, USA, Tech. Rep. NASA/TM-1999-209044, 1999.

[21] D. C. Ferguson, B. V. Vayner, and J. T. Galofaro, "Solar array arcing in LEO: How much charge is discharged?" in *Protection of Materials and Structures from the Space Environment*, J. I. Kleiman, Ed. New York, NY, USA: Springer-Verlag, 2006, pp. 9–19.

[22] A. Anders, "Perspective on the state-of-the-art for vacuum arcs and cathode processes," Presented at the 3rd Int. Workshop on Mechanisms of Vacuum Arcs, Albuquerque, NM, USA, Oct. 2012.

Dale C. Ferguson received the B.S. degree in astronomy from Case Western Reserve University, Cleveland, OH, USA, in 1970, and the Ph.D. degree in astronomy from the University of Arizona, Tucson, AZ, USA, in 1974.

He is the Lead for Spacecraft Charging Science and Technology at the Air Force Research Laboratory, Kirtland Air Force Base, Albuquerque, NM, USA. He was with the NASA Glenn Research Center, the NASA Marshall Space Flight Center, Arecibo Observatory, and the Max-Planck-Institut für Radioastronomie.

Boris V. Vayner received the M.S. degree in theoretical physics from Rostov State University, Rostov, Russia, the Ph.D. degree in astrophysics from the Institute of Astrophysics, Tartu, Estonia, and the Sc.D. degree in astrophysics and radio astronomy from Moscow State University, Moscow, Russia, in 1972, 1978, and 1991, respectively.

He was a Junior Researcher, Senior Researcher, and an Associate Professor with Rostov State University from 1972 to 1992. From 1994 to 1997, he was the National Research Council Fellow with the NASA Glenn Research Center, Space Environment Effects Branch. He is a Senior Scientist with the Ohio Aerospace Institute, Brook Park, OH, USA, in 1997. His current research interests include spacecraft-plasma interaction, low temperature plasma physics, and optical spectroscopy.